Structures of Leishmania major orthologues of macrophage migration inhibitory factor

Biochem Biophys Res Commun. Author manuscript; available in PMC 2011 December 18.

Published in final edited form as:
Biochem Biophys Res Commun. 2009 March 13; 380(3): 442–448. doi:10.1016/j.bbrc.2009.01.030.

STRUCTURAL CHARACTERISATION OF THE *LEISHMANIA MAJOR* ORTHOLOGUES OF MACROPHAGE MIGRATION INHIBITORY FACTOR (MIF)

Julia M. Richardson[1], **Lesley S. Morrison**[2], **Nicholas D. Bland**[2,3], **Sandra Bruce**[1], **Graham H. Coombs**[2,4], **Jeremy C. Mottram**[2], and **Malcolm D. Walkinshaw**[1]

[1]Structural Biochemistry Group, School of Biological Sciences, The King's Buildings, University of Edinburgh, Mayfield Road, Edinburgh EH9 3JR, Scotland. [2]Wellcome Centre for Molecular Parasitology and Division of Infection & Immunity, Faculty of Biomedical and Life Sciences, Glasgow Biomedical Research Centre, 120 University Place, Glasgow, G12 8TA, Scotland.

Abstract

Leishmania major, an intracellular parasitic protozoon that infects, differentiates and replicates within macrophages, encodes two closely related MIF-like proteins, which have only ~20% amino acid identity with mammalian MIF. Recombinant *L. major* MIF1 and MIF2 have been expressed and the structures, resolved by X-ray crystallography, show a trimeric ring architecture similar to mammalian MIF but with some structurally distinct features. LmjMIF1, but not LmjMIF2, has tautomerase activity, indicating that the LmjMIFs have evolved potentially different biological roles. This is further demonstrated by the differential life cycle expression of the proteins. LmjMIF2 is found in all life cycle stages whereas LmjMIF1 is found exclusively in amastigotes, the intracellular stage responsible for mammalian disease. The findings are consistent with parasite MIFs modulating or circumventing the host macrophage response and thereby promoting parasite survival, however analysis of the *L. braziliensis* genome showed that this species lacks intact *MIF* genes - highlighting that MIF is not a virulence factor in all species of *Leishmania*.

Parasites have adopted many strategies to avoid or subvert their hosts' immune responses including antigenic variation (1), signalling subversion (2) and immune evasion genes (3). *Leishmania* parasites are obligate intracellular pathogens and the causative agents of leishmaniases. The form and severity of the disease ranges from relatively mild dermal lesions to often fatal visceral infection depending on the infecting *Leishmania* species and the immune status of the host (4). *Leishmania* enter macrophages by receptor-mediated endocytosis (5) where they differentiate into amastigotes. A number of strategies are employed by the amistagotes to survive within parasitophorous vacuoles in host macrophages, including inhibition of NO production, hydrolytic enzymes and calcium chelation (6).

During the annotation of the *L. major* genome (7), two genes in tandem (*LmjMIF1* and *LmjMIF2*) were identified that encode proteins related to mammalian Macrophage Migration Inhibitory Factor (MIF), which is a major mediator of inflammatory processes (8). Increased serum levels of MIF contribute to a plethora of auto-immune diseases

Address correspondence to: JCM and MDW.
[3]Current address: Department of Biology (area 11), University of York, York, YO10 4YW, UK
[4]Current address: Strathclyde Institute of Pharmacy and Biomedical Sciences, University of Strathclyde, The John Arbuthnott Building, 27 Taylor Street, Glasgow G4 0NR, Scotland

Europe PMC Funders Author Manuscripts

including rheumatoid arthritis (9), type 2 diabetes (10) and colitis (11). Conversely, knock-out experiments in mice have shown that normal levels of MIF are required for the resolution of infections by *Salmonella typhimurium* (12), *Mycobacterium tuberculosis* (13), the helminth parasite *Taenia crassiceps* (14) and *L. major* (15). Macrophage activation by IFN-γ is prevented in MIF knockout mice, so that mice normally resistant to *L. major* develop non-healing leishmaniasis (15). Homologues of MIF are found in all mammalian genomes and some helminth parasites, such as *Trichinella spiralis* (16), *Ancylostoma ceylanicum* (17) and *Brugia malayi* (18). Helminth MIF-like proteins are postulated to modify host immune responses thus promoting parasite survival (19). Protozoan parasites including *Plasmodium falciparum, P. berghei* (20), and *Eimeria* species (21) also have characterised MIF orthologues that are released by the parasites to modulate the host immune system (22). MIF-like proteins are notably absent from African trypanosomes, which are closely related to *Leishmania* but do not infect macrophages.

There are now over 30 X-ray structures of MIF available from 8 species including, human (23), rat (24), mouse (25), frog (26) and the parasites *Brugia malayi* (27) and *L. major* (28) and this study). The trimeric architecture is maintained in all structures. Sequence identities among mammalian MIF sequences are high (above 85%) however this drops to 20-27% identity between the human and protozoan *Leishmania* and *Plasmodium* sequences. All of the structurally characterised MIF sequences show keto-enol tautomerase activity with model substrates like p-hydroxyphenylpyruvate and D-dopachrome, though the biological relevance of this well characterised activity is still unknown. Small molecule tautomerase inhibitors of mammalian MIF (29) are being developed for treatment of inflammatory diseases such as rheumatoid arthritis (30). Mammalian MIFs also have an oxidoreductase activity that is dependant on a CxxC thioredoxin-like motif. This motif is also implicated in the intracellular interaction of mammalian MIF with Jab-1, the catalytic subunit of the COP9 signalosome (31).

In this work we describe the X-ray structures of LmjMIF1 and LmjMIF2 and compare these structures with the known mammalian MIF structures. The possible biological roles of the two isoforms are discussed in relation to their structures and to their different enzyme activities.

EXPERIMENTAL PROCEDURES

Parasites

Leishmania major Friedlin (MHOM/JL/80/Friedlin) and *Leishmania braziliensis* (MHOM/BR/75M2904) were grown as promastigotes in modified Eagle's medium (designated HOMEM medium) supplemented with 10% heat inactivated foetal calf serum (FCS). *L. major* metacyclic promastigotes were isolated from stationary phase culture by agglutination of promastigote cells with peanut lectin as previously described (32). Lesion amastigotes were purified as previously described (33).

Multiple sequence alignment and phylogenetic reconstruction of MIF proteins

MIF-like protein sequences were identified by a BlastP search of Genbank at NCBI (http://www.ncbi.nlm.nih.gov/) using human MIF (CAG28572) as the query sequence. 60 sequences with significant blast scores were aligned using Tcoffee Expresso (http://tcoffee.vital-it.ch/cgi-bin/Tcoffee/tcoffee_cgi/index.cgi) using default settings (supplementary data 2). This alignment was subsequently used to generate a neighbour-joining phylogenetic tree using Mega 3.1 (http://www.megasoftware.net/). An unrooted circular tree lacking bootstrap values has been included in Figure 1, whereas a more detailed phylogram including percentage bootstrap values is included in supplementary data 3.

Cloning

L. major genes were amplified by PCR from genomic DNA isolated from promastigotes (reference strain MHOM/IL/80/Friedlin, zymodeme MON -103) using the DNeasy Tissue Kit (Qiagen). Mouse MIF was amplified from mouse cDNA prepared by Dr Peggy Shelbourne (Glasgow University) using whole brain tissue from C57BL/6J mice.

N-terminally his-tagged recombinant LmjF33.1740 (LmjMIF1) and LmjF33.1750 (LmjMIF2) were amplified using the following pairs of oligonucleotide primers containing artificial restriction sites (underlined): OL1820 *Nde*I (5′ GCATATGCCGGTCATTCAAACGTTTG) with OL1821 *Xho*I (5′ GGCTCGAGTTAGAAGTTTGTGCCATTCCAG) and OL 1822 *Nde*I (5′ GGCATATGCCGTTTCTGCAGACGATTG) with OL 1823 *Xho*I (5′ GGCTCGAGTCAAAAGTTAGTGCCGTTCCAG). The products were cloned into the *Nde*I/*Xho*I sites of pET28a (Novagen) to generate plasmids pGL1320 and pGL1319, respectively.

C-terminally his-tagged recombinant LmjMIF1, LmjMIF2 and mouse MIF (mMIF, Accession No. NM_010798) were amplified using the following pairs of oligonucleotide primers containing artificial restriction sites (underlined): OL1820 with OL 2062 *Xho*I (5′ GGCTCGAGGAAGTTTGTGCCATTCCAG), OL1822 with OL 2063 *Xho*I (5′ GGCTCGAGAAAGTTAGTGCCGTTCCAG) and OL 2230 *Nde*1 (5′ CATATGCCTATGTTCATCG) with OL2231 *Xho*I (5′ CTCGAGAGCGAAGGTGGAACCG). The products were cloned into the *Nde*I/*Xho*I sites of pET21a (Novagen) to give plasmids pGL1504, pGL1505 and pGL1574, respectively. P1G mutants were made in accordance with the QuikChange® Site-Directed Mutagenesis Kit (Stratagene) with pGL1504 and pGL1505 as template DNA and the following pairs of degenerate (underlined) primers: OL2070 (CCTCAGCGAAAATGGGGGTCATTCAAACG) with OL2071 (CGTTTGAATGACCCCCATTTTCGCTGAGG) to create pGL1506 (LmjMIF1^{P1G}) and OL2072 (CCCACCTAAGAAAATGGGGTTTCTGCAGACG) with OL2073 (CGTCTGCAGAAACCCCATTTTCTTAGGTGGG) to create pGL1507 (LmjMIF2^{P1G}).

The LmjMIF locus including flanking regions was amplifiied using the following pair of oligonucleotide primers containing artificial restriction sites (underlined): OL2033 *Not*1 (5′ GCGGCCGCGCGCCACCCCAATAG) and OL 2003 *Xho*1 (AGATCTAAGGATGCAATTATGTAG) and PFx50™ polymerase (Invitrogen) and cloned into the pRIB expression vector (34) to give pGL1540. All plasmids were sequenced in both directions, to confirm the integrity of the constructs.

Recombinant protein expression and purification

Plasmids were transformed into BL21(DE3) cells for recombinant protein expression. Recombinant LmjMIF and mouse MIF were induced with IPTG (1 mM) at 30°C and 37°C, respectively. Cells were grown in 1 L cultures and the induced protein expression continued overnight. Following cell lysis by sonication in 20 mL of NaH_2PO_4/300 mM NaCl pH 8.0 containing 10 μg mL^{-1} DNAase and 100 μg mL^{-1} lysozyme, the supernatant was filtered and recombinant proteins purified using Nickel chelate chromatography followed by desalting and HQ ion exchange chromatography. Proteins were concentrated to ~13 mg mL^{-1} and stored in 50 mM Tris, 5 mM EDTA pH 7.0 at 4°C for up to 3 months without loss of activity.

Crystallisation

Crystals were grown by the hanging drop, vapour diffusion method in 24-well Linbro plates. Crystals of LmjMIF1 grew in 3-5 days to a maximum size of 0.2 × 0.2 × 0.4 mm at 290 K under the following conditions: the well contained 30% (*w/v*) PEG 4000, 100 mM imidazole pH 6.5 and the drop contained 2 μL of protein solution at 13 mg mL^{-1} plus 2 μL of well solution. Hexagonal plate-like crystals of LmjMIF2 grew at 290 K in drops containing 2 μL of protein at 17 mg mL^{-1} and 2 μL of well solution, consisting of 29% (*w/v*) PEG 4000 and 100 mM Hepes, pH 7.5. Prior to data collection, crystals were flash frozen in liquid nitrogen directly from the well solution.

X-ray data collection and structure determination

All data were collected on beamline BM14 at the ESRF (Grenoble, France) on a MAR CCD detector using a ϕ scan with a step size of 1°. Data indexing was performed using Mosflm and the merging and scaling was carried out with SCALA (35). Data statistics are shown in Table 1. Molecular replacement was performed with the program MOLREP (within the CCP4 software suite (35)) using the structure of *Xenopus laevis* MIF (PDBID:1UIZ) as the search model - it has 26% and 28% sequence identity to LmjMIF1 and LmjMIF2, respectively. Structure building and refinement was performed using COOT (36) and Refmac, respectively.

Enzyme assays

Tautomerase activity was assayed as previously described (37). All reactions were carried out in a total volume of 800 μl at 37°C. The tautomerase substrate L-dopachrome methyl ester was generated by adding 48 μL of L-dopa methyl ester (10 mM) and 32 μL of sodium periodate (20 mM) to an appropriate volume of 10 mM sodium phosphate (pH 6.2) with 1 mM EDTA. For inhibition assays, 10 μL of ISO-1 (10 mM, Merck Biosciences, UK) or DMSO was also added. The spontaneous decay of L-dopachrome methyl ester was measured by absorbance (λ_{474} nm) using a Hewlett Packard 8453 UV/Visible spectrophotometer for 30 s prior to the addition of recombinant protein. Specific activity was determined using $\varepsilon = 3700\ M^{-1}\ cm^{-1}$.

MIF oxidoreductase activity was assayed in 200 mM sodium phosphate (pH 7.2) with 0.5 mg mL^{-1} insulin and 20 mM glutathione (Sigma, UK) at 37°C. Mouse MIF, LmjMIF1 and LmjMIF2 (200 μg) were added and reduction of insulin was measured by the increase of absorbance (λ_{650} nm) using a Hewlett Packard 8453 UV/Visible spectrophotometer. The rate of reduction by MIFs was found relative to the intrinsic rate of insulin reduction by glutathione (control).

Antibodies and Western analyses

Purified recombinant LmjMIF1 and LmjMIF2 were used to raise antisera in rabbits. Antibodies were purified from sera using recombinant protein immobilized onto AminoLink Plus coupling gel (Pierce). *Leishmania* cell pellets from all life cycle stages were lysed in 2% SDS containing protease inhibitor cocktail (Boehringer), protein concentration was determined by Bradford Assay and extracts stored at −20°C until required. Samples containing 10 μg of total protein were prepared using 4 x sample buffer and water, to equalise loading volumes, prior to incubation at 95°C for 4 min to denature the protein. Polyacrylamide electrophoresis was performed using a 12% gel run at 200V for ~45 min in NuPAGE™ MES running buffer. Proteins were transferred to a nitrocellulose membrane and detected using primary antibody diluted 1 in 1000 in TBST, secondary anti-rabbit IgG coupled to HRP conjugate (Santa Cruz Biotechnology) and chemiluminescent substrate (Pierce).

Generation of transgenic L. braziliensis

Plasmid pGL1540 was digested with *Pme*1/*Pac*1, to remove the integration cassette which was gel purified. Transfections were carried out using a human T-cell Amaxa nucleofector kit (Amaxa Biosystems) according to the manufacturer's protocol. 5×10^7 mid-log phase *L. braziliensis* were harvested at 1000 × g for 10 min and resuspended in 100 μL of buffer for Human T-cells and electroporated with 10 μg of the purified pGL1540 DNA using the U-33 programme before being transferred to 10 mL of fresh HOMEM medium with 10% (*v/v*) HIFCS. 10 mL cultures were split into two 5 mL cultures to select for independent transfection events and incubated at 25°C overnight. The following day, puromycin was added to a final concentration of 50 μg mL^{-1} and serial dilutions were performed to select for transfected clones. Cells were plated out in 96-well plates and incubated at 25°C.

Macrophage infection assays

Peritoneal macrophages form BALB/c mice were collected following injection of 5 mL of ice-cold RPMI 1640-medium into the peritoneal cavity and gentle massage. Macrophages were counted and re-suspended at a density of 5×10^5 cells mL^{-1} in RPMI supplemented with 10% (*v/v*) HIFCS. 100μL of macrophage suspension were added to each well of a 16-well Lab-tek™ cavity slide (50k mΦ/well) and incubated at 37°C, 5% CO_2 overnight. Cells were washed and incubated with stationary phase promastigotes at a 10:1 ratio for 24hrs at 37°C. Later time points were given fresh media every 24 hours and incubated as before. After incubation, slides were fixed with 70% methanol, Geimsa stained and the number of infected cells determined by visualization under a light microscope.

RESULTS and DISCUSSION

Sequence alignments and phylogenetic reconstruction

A phylogenetic tree of evolutionary relationships was generated from the multiple sequence alignment of 60 MIF-like proteins using a neighbour-joining algorithm (Figure 1A). This tree was highly parsimonious with known evolutionary relationships. Strong clades delineate along known taxonomic lines, the main clusters being cyanobacteria, nematodes, vertebrates, apicomplexans (with *Giardia*) and plants. A strong association is seen between MIFs from *L. major, L. infantum and L. mexicana* and gram positive bacteria belonging to the genera *Bifidobacterium* and *Clostridium. L. braziliensis* was found not to contain intact *MIF1* or *MIF2* genes (see below). The broad taxonomic distribution of *MIF*-like genes is indicative of the ancient lineage of these proteins. It also appears that gene deletion events are common for this family, for example MIF-like proteins are common in nematodes but there are none in *Drosophila melanogaster*. However, the presence of the *Leishmania* MIFs in a paraphyletic cluster, showing a strong association with bacterial MIF-like proteins, is the only example of such an association in the analysis; this may be indicative of a lateral gene transfer event (38).

Leishmania often have tandem repeats of genes that serve to increase the ultimate expression of encoded proteins (38). On initial analysis it appeared that in *L. major* the two tandem copies of MIF were an example of this, however, they are likely to be two independent genes (*LmjMIF1* and *LmjMIF2*) that have undergone distinct directional selection subsequent to a gene duplication event. The presence of two MIFs in *Leishmania* is unusual in that with the exception of some nematode species MIF orthologues are found as a single copy, suggesting unique functions for these proteins. The *L. major*, *L. mexicana* and *L. infantum* genomes contain *MIF1* and *MIF2*-like genes that have 96-99% and 95-96% amino acid identity, respectively. MIF1 and MIF2 sequences within a species have ~58% amino acid identity to each other, and each has ~20% identity with mouse MIF. Alignment of the sequences of LmjMIF1, LmjMIF2 with *Brugia malayi*, human and mouse MIF proteins

(Figure 1B) reveals the conservation in LmjMIFs of the essential N-terminal proline residue and a GKP motif (residues 32-34) involved in the tautomerase active site (39). The proline of the GKP motif is replaced by Ser in the gram positive bacteria MIF sequences (Figure 1B). The CxxC motif, implicated in oxidoreductase activity of the human enzyme (residues 55 to 59) (31), is not found in either of the LmjMIFs.

LmjMIF1 has tatutomerase activity, LmjMIF2 is inactive

Recombinant LmjMIF1 and LmjMIF2 were produced with either N- or C-terminal histidine tags. Recombinant N-terminal his-tagged LmjMIF1 and LmjMIF2 lacked enzymatic activity, so C-terminal his-tagged proteins were used for enzyme assays. LmjMIF1 demonstrated a tautomerase activity that was 26-fold lower than that of mouse MIF (Table 2), whereas LmjMIF2 was unable to tautomerase L-dopachrome methyl ester. The specific activity of LmjMIF1 (0.36 mM min^{-1} μM^{-1}) compares with a previously reported value of 3.35 mM min^{-1} μM^{-1} for human MIF (28). Mutation of the catalytic proline of LmjMIF1 to a glycine ($LmjMIF1^{P1G}$) ablated tautomerase activity (Table 2). Mouse MIF tautomerase activity was completely inhibited by 1.25 mM ISO-1 (IC_{50}=10.5 μM), however LmjMIF1 tautomerase activity was unaffected by this concentration of inhibitor. Mouse MIF has oxidoreductase activity (31) and LmjMIF1 has a small, but detectable activity, whilst no oxidoreductase activity was detected with LmjMIF2 (Supplementary data 4). The absence of this activity is not surprising given that the LmjMIFs do not contain the CxxC motif required for mammalian oxidoreductase activity. The low level of activity shown by LmjMIF1 may be due to the presence of a cysteine residue, absent in LmjMIF2, located in the vicinity of the CxxC motif (Figure 1B). Bacterial orthologues of mammalian MIFs also lack the CxxC motif and it is likely that oxidoreductase activity evolved during the evolution of MIFs in eukaryotes.

Crystal structures of LmjMIF1 and LmjMIF2

Crystal structures of three LmjMIF1 and LmjMIF2 proteins have been determined: LmjMIF1 with an N-terminal hexa-his tag (N-His-LmjMIF1) to 1.8 Å resolution, LmjMIF2 with an N-terminal hexa-his tag (N-His-LmjMIF2) to 1.9 Å resolution and LmjMIF1 with a C-terminal hexa-his tag (C-His-LmjMIF1) to 2.6 Å resolution. Data collection and refinement statistics are given in Table 1. All three structures were solved using molecular replacement with a model based on the structure of *Xenopus* MIF (1UIZ) which, of the structures solved, has the closest amino acid sequence identity (28.9 % and 28.4 %) to the *L. major* sequences. The LmjMIF proteins adopt a trimeric ring architecture (Figure 2A,B) similar to the other known MIF structures (Figure 2C) with each monomer composed of a 4-stranded mixed β-sheet and two α-helices stacked against the β-sheet on the outside of the trimer.

The recently published structure of LmjMIF1 (28) has a hexagonal unit cell with dimensions a=b=52.32 Å, c=96.82 Å which is closely isomorphous with the N-His-LmjMIF1 crystal form obtained in this work (a,b=52.32Å, c=97.94Å). No interpretable electron density for the N-terminal tag was found in this structure. A least squares fit of the refined structure of N-His-LmjMIF1 gave an r.m.s.d. for all residues of 0.4 Å. Thus, despite different crystallisation conditions and different expression constructs, it appears that the two structures are essentially identical. The C-His-LmjMIF1 construct, used for enzymatic assays, was also found to adopt an essentially identical trimeric structure with r.m.s.d. fits for the complete trimer to 3B64 (28) of 0.4 Å and N-His-LmjMIF of 0.6 Å. (Figure 2D).

LmjMIF1 and LmjMIF2 have structural differences

N-His-LmjMIF2 shows some structural features that differ subtly from N-His-LmjMIF1. Individual chains of the LmjMIF1 and LmjMIF2 monomers can be superimposed with an

r.m.s.d. of 0.9 Å for all Cα atoms and differ only in the conformation of residues 30 to 37 (30VLGKPEDL37 in LmjMIF1 and 30ELGKPEDF37 in LmjMIF2), which link the C-terminal end of the first helix α1 with the second strand (β2) of the 4-stranded sheet. This linker loop contains the active site residue K33 within the conserved GKP motif. In LmjMIF1, the four residues 34PEDL37 form a β-turn (Figure 2E) while in LmjMIF2 a turn-like conformation is adopted by the four residues 33KPED36 (Figure 2F). In the N-His-MIF1 and 3B64 structures, the conformation of this motif which locks the side chain of K33 in the vicinity of the P1 is in part determined by salt bridges between R24 and D36 and R28 and E35, where R24 and R28 lie in the middle of α1 and are separated by one turn of the long helix. These residues are conserved among the *Leishmania* MIFs, except LmMIF2 where there is an R24G mutation. The LmjMIF2 structure accommodates the removal of such a large side chain, which abuts the 4-stranded sheet by partially filling this space with the side chain of F37. The significant conformational change in this conserved sequence places K33 away from P1, which has a likely adverse affect on the mechanism (see below). The structural analysis is complicated in this instance by the presence of N-terminal His-tag residues attached to P1. However modelling shows that these residues would not prevent the 31LGKPED36 motif adopting the same conformation as found in the LmjMIF1 structures and that the likely driver for the conformational change (and loss of tautomerase activity) is the R24G difference in sequence.

LmjMIF structures differ in two key regions from all other MIF structures

Comparison of the trimer structures of LmjMIF1 and LmjMIF2 with MIF structures from the other available species shows that both LmjMIF1 and LmjMIF2 are the most distinct. A least squares fit using α-carbons from all three chains in the trimer gives r.m.s.d values of around 4Å against the vertebrate (200W, 1MFF, 1FIM) and helminth (1HFO) structures. The r.m.s. fit among these vertebrate and helminth trimer structures is only around 1Å. It is also worth noting that the these rms deviations are almost the same whether individual chains (about 110 C-α atoms) or the complete trimer of 330 C-α atoms are used for the fit. This suggests that there is no inter-domain flexibility in the trimer as can be found in other homo-oligomeric enzymes, e.g. pyruvate kinase (40).

A comparison of LmjMIF2 with mammalian MIF (2OOW and 1MFF) identified two regions with structural differences. The first helix (α1) extends from residues 13 to 31 in both LmjMIF structures while it is significantly shorter in all structures from other species (Figure 3). In mouse and human, for example, α1 extends from residues 18 to 30. All MIF structures from mammalian and invertebrates also have a short η1 helix (residues 10-14) with a conserved Pro15 acting as a helix breaker between η1 and α1; this is located on the bottom face of the trimer, distal from the tautomerase active site. There is a conserved change in sequence in the *L. major* MIFs (Pro15Lys) and a concomitant disappearance of η1 and lengthening of α1. The change in helix length has a quite significant effect on the position of α1 in the *L. major* structures relative to the other MIF structures (Figure 4A). It is likely that this change in helix position is a major contributor to the rather poor r.m.s. fit between LmjMIFs and the other structures.

The second region of the LmjMIFs that differs significantly from all other MIF structures is on the top surface of the trimer close to the tautomerase active site and comprises the loop between residues 64 and 71 (which joins the strand β4 with the second long helix α2) and residues 100 to107 which continue from strand β5 (Figure 3B). The sequence of the 64-71 loop differs in the two *L. major* proteins (64ALGGYGPS71 in LmjMIF1 and 64SWGEYAPS71 in LmjMIF2) but they have similar conformations. However, an overlay of the 64-71 loop from the *L. major* and mouse MIF structures shows that corresponding main chain atoms are over 6 Å apart. An active site residue at the beginning of this loop (Ile64 in mouse MIF, Leu65 in LmjMIF1 and Trp65 in LmjMIF2) plays an important role in

substrate recognition and is shifted away the active site in the LmjMIF2 structure. Most 64-71 loops (with the notable exception of LmjMIF2) have a total of three Gly residues within this short sequence, and Gly66 is absolutely conserved through all MIF sequences implying that flexibility of the loop is important for either substrate recognition or enzymatic activity. Strand β5 is extended in the *L. major* MIFs compared to other MIFs and the sequence continues into strand β6 (residues 103 to 107) whereas a turn (η4) forms in mammalian MIFs (Figure 3B). This difference in conformation leads to a narrower pore on the top face of the trimer in the *L. major* MIFs.

A comparison of the electrostatic surfaces (Figure 4) shows the mammalian MIFs have a very positively charged top trimer face, which is similar to LmjMIF2. This contrasts with the predominantly negative surface of LmjMIF1. These images also highlight the central hole in the MIF trimer, which has a rather variable size depending on sequence. The hydrophobic hole of the human MIF is large enough to accept an extended hydrocarbon chain, such as a lipopolysaccharide (LPS) molecule (8). It is less likely that such an interaction is relevant to the biology of *Leishmania* – and indeed the hole in the LmjMIF trimer provides a less good fit for LPS.

The tautomerase active site

The keto-enol tautomerase active site of mouse MIF is formed by Pro1, Lys32 and Ile64 of one monomer and Tyr95 and Asn97 of the adjacent monomer (39). The N-terminal Pro1 is the general base catalyst in the reaction and Lys33 plays a role in lowering the pKa of this residue as well as binding the substrate (39). These two residues are conserved in the *L. major* MIFs, and their positions are also conserved in the LmjMIF1 structure (Table 3, Figure 2A). However in LmjMIF2 the different conformation of the turn spanning L31-D36 displaces the side-chain of Lys33 away from the active site, thus affecting its catalytic role (Figure 2B). The change in the active site structure of LmjMIF2 may affect the entry of the substrate to the ligand binding pocket.

The third tautomerase active site residue of both LmjMIF1 and LmjMIF2 (L65 and W65, respectively) have subtly different positions compared with the equivalent residue in mouse MIF (I64), due to the different conformation of the loop formed by residues 64 to 71 and the presence of β6 in place of η4. The fourth and fifth active site residues are not essential for mouse MIF tautomerase activity: the mutants Y95F and N97A had no effect on activity (41), but the latter showed reduced inhibitor binding affinity. N97 is replaced by hydrophobic residues in the *L. major* MIFs (Table 3) which would be unable to form stabilising hydrogen bonds with a substrate. Moreover, the bulky side-chain of F98 in LmjMIF2 may reduce the size of the active site. Resolution of the LmjMIF tertiary structures thus reveal subtle but potentially significant structural differences not only between mammalian MIF and the LmjMIFs but between the individual parasite proteins, which may explain the observed differences of LmjMIF enzyme activities.

LmjMIF1 has significantly less tautomerase activity than mouse MIF and LmjMIF2 was inactive. L-dopachrome, however, is not a physiological substrate of MIFs and so inability to utilise it as a substrate does not provide definitive evidence for LmjMIF2 being inactive. Nevertheless, this is highly indicative of the two LmjMIFs having differential substrate specificities. It is also interesting to note that ISO-1, an inhibitor of mammalian MIF, does not inhibit LmjMIF1, thus suggesting that there may be opportunity to design MIF species-specific inhibitors.

Species- and stage-specific expression of MIF1 and MIF2

Analysis of the *L. braziliensis* genome (www.genedb.org) indicates that this species lacks intact *MIF* genes. To confirm this, the MIF locus was PCR amplified from the genome strain (*L. braziliensis* M2904) and sequenced. This showed that the region around the MIF locus had maintained synteny with the other *Leishmania* species (Figure 5A), but that the *MIF* genes had undergone a process of pseudogene formation. *MIF1* is truncated by a frame shift, while a deletion has removed the start codon for *MIF2* (Figure 5A). This was confirmed by western blot analysis (Figure 5B, lane 2) as neither MIF1 nor MIF2 could be detected in protein extracts from *L. braziliensis* promastigotes with anti-MIF antibody, although the antibodies detected *L. mexicana* and *L. infantum* MIF1 and MIF2 (data not shown).

Affinity purified rabbit anti-LmjMIF1 antibody was found to be specific for LmjMIF1 (Figure 5C, lane 1) as it does not react with recombinant LmjMIF2 (rLmjMIF2), lane 2). In contrast, the anti-LmjMIF2 antibody displays some cross reactivity as it recognises rLmjMIF1 and rLmjMIF2 (Figure 5C, lanes 1 and 2, lower panel). LmjMIF1 was only expressed in *L. major* amastigotes (Figure 5C, lane 5) while LmjMIF2 was expressed during all the life cycle stages analysed namely procyclic promastigote, the flagellated replicative form of the parasite found in the abdominal midgut of the sandfly; metacyclic promastigote, the mammalian infective form found in sandfly mouth parts and intracellular amastigote, resident in mammalian host macrophages (Figure 5C, lanes 3-5). The stage-specific expression pattern of the LmjMIFs is a further indication that they have different biological roles.

When *LmjMIF1* and *LmjMIF2* were introduced into the ribosomal locus of *L. braziliensis*, expression of both MIF proteins could be detected by western blot in the promastigote life cycle stage (Figure 5B, lanes 3, 4 and 5). To test if expression of *L. major* MIF genes in *L. braziliensis* influenced the ability of the parasites to infect host cells, a macrophage infection assay was performed. This showed that the combined expression of both LmjMIFs in *L. braziliensis* increased the level of infection by 20% in comparison to wild type *L. braziliensis* (Figure 5D). It did not, however, increase the ability of the parasites to survive within macrophages as levels of infection of the transgenic parasites declined in line with wild type *L. braziliensis* by day 5 of the infection. While the absence of MIF from *L. braziliensis* shows that MIF is not required for infection in all *Leishmania* species, it highlights the intriguing possibility that *Leishmania* MIFs have a role in disease tropism or may contribute to disease severity and outcome in conjunction with a host's own immune responses (42). Host genetics and in particular IL-6 (43) and IL-10 (44) polymorphisms are associated with mucosal and both mucosal and cutaneous leishmaniasis respectively and studies have linked regions on human chromosomes 15 and 19 with protection from visceral leishmaniasis (45). Parasite genetics also contribute to the clinical outcome of leishmaniasis and levels of protein expression can significantly alter tissue tropism and disease severity (46).

Perspective

More studies involving immunological analyses using transgenic parasites are required to determine the role of MIF proteins in *L. major*, but it seems likely that at least the amastigote-specific MIF1 is involved in host-parasite interactions. This is a hypothesis further strengthened by the recent publication of the *L. donovani* promastigote 'secretome' (47). The secretome consists of parasite proteins that are actively secreted from *L. donovani* promastigotes, this clearly misses amastigote-specific proteins – which accounts for the absence of LdMIF1. However LdMIF2 was identified, which is consistent with a role in the insect infective stages of the parasite.

Although the exact role of mammalian MIF in inflammation and immune response is currently controversial, it is increasingly evident that some intracellular parasites, including *Plasmodium*, have MIF-like proteins that are likely to be involved in immune invasion and can be detected in host sera (48). This physical characterisation of the LmjMIF proteins has shown that they are structurally, biochemically and temporally capable of contributing to *Leishmania* parasite persistence. Further *in vivo* biological analysis is underway to elucidate their precise roles.

Supplementary Material

Refer to Web version on PubMed Central for supplementary material.

Acknowledgments

We thank Alan Scott for help with protein purification and Chi Chan for help with the *L. braziliensis* analysis. This work was funded by the Medical Research Council [grant numbers G9722968, G0000508, G0700127] and The Wellcome Trust [grant number 074522].

REFERENCES

1. Palmer GH, Brayton KA. Trends in Parasitology. 2007; 23:408–413. [PubMed: 17662656]
2. Olivier M, Gregory DJ, Forget G. Clin. Microbiol. Rev. 2005; 18:293–305. [PubMed: 15831826]
3. Maizels RM, Gomez-Escobar N, Gregory WF, Murray J, Zang X. International Journal for Parasitology. 2001; 31:889–898. [PubMed: 11406138]
4. Cunningham AC. Experimental and Molecular Pathology. 2002; 72:132–141. [PubMed: 11890722]
5. Alexander J, Satoskar AR, Russell DG. J. Cell Sci. 1999; 112:2993–3002. [PubMed: 10462516]
6. Descoteaux A, Matlashewski G, Turco SJ. J. Immunol. 1992; 149:3008–3015. [PubMed: 1383336]
7. Ivens AC, Peacock CS, Worthey EA, Murphy L, Aggarwal G, Berriman M, Sisk E, Rajandream MA, Adlem E, Aert R, Anupama A, Apostolou Z, Attipoe P, Bason N, Bauser C, Beck A, Beverley SM, Bianchettin G, Borzym K, Bothe G, Bruschi CV, Collins M, Cadag E, Ciarloni L, Clayton C, Coulson RMR, Cronin A, Cruz AK, Davies RM, De Gaudenzi J, Dobson DE, Duesterhoeft A, Fazelina G, Fosker N, Frasch AC, Fraser A, Fuchs M, Gabel C, Goble A, Goffeau A, Harris D, Hertz-Fowler C, Hilbert H, Horn D, Huang Y, Klages S, Knights A, Kube M, Larke N, Litvin L, Lord A, Louie T, Marra M, Masuy D, Matthews K, Michaeli S, Mottram JC, Muller-Auer S, Munden H, Nelson S, Norbertczak H, Oliver K, O'Neil S, Pentony M, Pohl TM, Price C, Purnelle B, Quail MA, Rabbinowitsch E, Reinhardt R, Rieger M, Rinta J, Robben J, Robertson L, Ruiz JC, Rutter S, Saunders D, Schafer M, Schein J, Schwartz DC, Seeger K, Seyler A, Sharp S, Shin H, Sivam D, Squares R, Squares S, Tosato V, Vogt C, Volckaert G, Wambutt R, Warren T, Wedler H, Woodward J, Zhou S, Zimmermann W, Smith DF, Blackwell JM, Stuart KD, Barrell B, Myler PJ. Science. 2005; 309:436–442. [PubMed: 16020728]
8. Kudrin A, Scott M, Martin S, Chung C. w. Donn R, McMaster A, Ellison S, Ray D, Ray K, Binks M. J. Biol. Chem. 2006; 281:29641–29651. [PubMed: 16893895]
9. Leech M, Metz C, Bucala R, Morand EF. Arthritis and Rheumatism. 2000; 43:827–833. [PubMed: 10765927]
10. Yabunaka N, Nishihira J, Mizue Y, Tsuji M, Kumagai M, Ohtsuka Y, Imamura M, Asaka M. Diabetes Care. 2000; 23:256–258. [PubMed: 10868843]
11. de Jong YP, Abadia-Molina AC, Satoskar AR, Clarke K, Rietdijk ST, Faubion WA, Mizoguchi E, Metz CN, Sahli MA, ten Hove T, Keates AC, Lubetsky JB, Farrell RJ, Michetti P, van Deventer SJ, Lolis E, David JR, Bhan AK, Terhorst C. Nat Immunol. 2001; 2:1061–1066. [PubMed: 11668338]
12. Koebernick H, Grode L, David JR, Rohde W, Rolph MS, Mittrucker HW, Kaufmann SHE. PNAS. 2002; 99:13681–13686. [PubMed: 12271144]
13. Oddo M, Calandra T, Bucala R, Meylan PRA. Infect. Immun. 2005; 73:3783–3786. [PubMed: 15908412]

14. Rodriguez-Sosa M, Rosas LE, David JR, Bojalil R, Satoskar AR, Terrazas LI. Infect. Immun. 2003; 71:1247–1254. [PubMed: 12595439]
15. Satoskar AR, Bozza M, Sosa M. Rodriguez, Lin G, David JR. Infect. Immun. 2001; 69:906–911. [PubMed: 11159984]
16. Tan TH, Edgerton SA, Kumari R, McAlister MS, Roe SM, Nagl S, Pearl LH, Selkirk ME, Bianco AE, Totty NF, Engwerda C, Gray CA, Meyer DJ, Rowe SM. Biochem. J. 2001; 357:373–383. [PubMed: 11439086]
17. Cho Y, Jones BF, Vermeire JJ, Leng L, DiFedele L, Harrison LM, Xiong H, Kwong YKA, Chen Y, Bucala R, Lolis E, Cappello M. J. Biol. Chem. 2007; 282:23447–23456. [PubMed: 17567581]
18. Zang X, Taylor P, Wang JM, Meyer DJ, Scott AL, Walkinshaw MD, Maizels RM. J. Biol. Chem. 2002; 277:44261–44267. [PubMed: 12221083]
19. Pastrana DV, Raghavan N, FitzGerald P, Eisinger SW, Metz C, Bucala R, Schleimer RP, Bickel C, Scott AL. Infect. Immun. 1998; 66:5955–5963. [PubMed: 9826378]
20. Augustijn KD, Kleemann R, Thompson J, Kooistra T, Crawford CE, Reece SE, Pain A, Siebum AHG, Janse CJ, Waters AP. Infect. Immun. 2007; 75:1116–1128. [PubMed: 17158894]
21. Miska KB, Fetterer RH, Lillehoj HS, Jenkins MC, Allen PC, Harper SB. Mol. Biochem. Parasitol. 2007; 151:173–183. [PubMed: 17194492]
22. Cordery D, Kishore U, Kyes S, Shafi M, Watkins K, Williams T, Marsh K, Urban B. The Journal of Infectious Diseases. 2007; 195:905–912. [PubMed: 17299722]
23. Sun HW, Bernhagen J, Bucala R, Lolis E. Proc. Natl. Acad. Sci. U. S. A. 1996; 93:5191–5196. [PubMed: 8643551]
24. Suzuki M, Sugimoto H, Nakagawa A, Tanaka I, Nishihira J, Sakai M. Nat. Struct. Biol. 1996; 3:259–266. [PubMed: 8605628]
25. Taylor AB, Johnson WH Jr. Czerwinski RM, Li HS, Hackert ML, Whitman CP. Biochemistry. 1999; 38:7444–7452. [PubMed: 10360941]
26. Suzuki M, Takamura Y, Maeno M, Tochinai S, Iyaguchi D, Tanaka I, Nishihira J, Ishibashi T. J. Biol. Chem. 2004; 279:21406–21414. [PubMed: 15024012]
27. Zang X, Taylor P, Wang JM, Meyer DJ, Scott AL, Walkinshaw MD, Maizels RM. J. Biol. Chem. 2002; 277:44261–44267. [PubMed: 12221083]
28. Kamir D, Zierow S, Leng L, Cho Y, Diaz Y, Griffith J, McDonald C, Merk M, Mitchell RA, Trent J, Chen Y, Kwong YK, Xiong H, Vermeire J, Cappello M, Mahon-Pratt D, Walker J, Bernhagen J, Lolis E, Bucala R. J. Immunol. 2008; 180:8250–8261. [PubMed: 18523291]
29. Al Abed Y, Dabideen D, Aljabari B, Valster A, Messmer D, Ochani M, Tanovic M, Ochani K, Bacher M, Nicoletti F, Metz C, Pavlov VA, Miller EJ, Tracey KJ. J. Biol. Chem. 2005; 280:36541–36544. [PubMed: 16115897]
30. Morand EF, Leech M, Bernhagen J. Nat Rev Drug Discov. 2006; 5:399–411. [PubMed: 16628200]
31. Kleemann R, Kapurniotu A, Frank RW, Gessner A, Mischke R, Flieger O, Juttner S, Brunner H, Bernhagen J. J. Mol. Biol. 1998; 280:85–102. [PubMed: 9653033]
32. Ready PD, Smith DF. Trans. R. Soc. Trop. Med. Hyg. 1988; 82:418. [PubMed: 3232177]
33. Hart DT, Vickerman K, Coombs GH. Parasitology. 1981; 82:345–355. [PubMed: 7243344]
34. Garami A, Ilg T. EMBO J. 2001; 20:3657–3666. [PubMed: 11447107]
35. Acta Crystallogr. D. Biol. Crystallogr. 1994; 50:760–763. [PubMed: 15299374]
36. Emsley P, Cowtan K. Acta Crystallogr. D. Biol. Crystallogr. 2004; 60:2126–2132. [PubMed: 15572765]
37. Pennock JL, Behnke JM, Bickle QD, Devaney E, Grencis RK, Isaac RE, Joshua GW, Selkirk ME, Zhang Y, Meyer DJ. Biochem. J. 1998; 335:495–498. [PubMed: 9794786]
38. Peacock CS, Seeger K, Harris D, Murphy L, Ruiz JC, Quail MA, Peters N, Adlem E, Tivey A, Aslett M, Kerhornou A, Ivens A, Fraser A, Rajandream MA, Carver T, Norbertczak H, Chillingworth T, Hance Z, Jagels K, Moule S, Ormond D, Rutter S, Squares R, Whitehead S, Rabbinowitsch E, Arrowsmith C, White B, Thurston S, Bringaud F, Baldauf SL, Faulconbridge A, Jeffares D, Depledge DP, Oyola SO, Hilley JD, Brito LO, Tosi LRO, Barrell B, Cruz AK, Mottram JC, Smith DF, Berriman M. Nat Genet. 2007; 39:839–847. [PubMed: 17572675]

39. Lubetsky JB, Swope M, Dealwis C, Blake P, Lolis E. Biochemistry. 1999; 38:7346–7354. [PubMed: 10353846]
40. Tulloch LB, Morgan HP, Hannaert V, Michels PA, Fothergill-Gilmore LA, Walkinshaw MD. J. Mol. Biol. 2008
41. Stamps SL, Taylor AB, Wang SC, Hackert ML, Whitman CP. Biochemistry. 2000; 39:9671–9678. [PubMed: 10933783]
42. Peacock CS, Seeger K, Harris D, Murphy L, Ruiz JC, Quail MA, Peters N, Adlem E, Tivey A, Aslett M, Kerhornou A, Ivens A, Fraser A, Rajandream MA, Carver T, Norbertczak H, Chillingworth T, Hance Z, Jagels K, Moule S, Ormond D, Rutter S, Squares R, Whitehead S, Rabbinowitsch E, Arrowsmith C, White B, Thurston S, Bringaud F, Baldauf SL, Faulconbridge A, Jeffares D, Depledge DP, Oyola SO, Hilley JD, Brito LO, Tosi LR, Barrell B, Cruz AK, Mottram JC, Smith DF, Berriman M. Nat. Genet. 2007; 39:839–847. [PubMed: 17572675]
43. Castellucci L, Menezes E, Oliveira J, Magalhaes A, Guimaraes LH, Lessa M, Ribeiro S, Reale J, Noronha EF, Wilson ME, Duggal P, Beaty TH, Jeronimo S, Jamieson SE, Bales A, Blackwell JM, de Jesus AR, Carvalho EM. J. Infect. Dis. 2006; 194:519–527. [PubMed: 16845637]
44. Salhi A, Rodrigues V Jr. Santoro F, Dessein H, Romano A, Castellano LR, Sertorio M, Rafati S, Chevillard C, Prata A, Alcais A, Argiro L, Dessein A. J. Immunol. 2008; 180:6139–6148. [PubMed: 18424735]
45. Jeronimo SM, Duggal P, Ettinger NA, Nascimento ET, Monteiro GR, Cabral AP, Pontes NN, Lacerda HG, Queiroz PV, Gomes CE, Pearson RD, Blackwell JM, Beaty TH, Wilson ME. J. Infect. Dis. 2007; 196:1261–1269. [PubMed: 17955446]
46. Zhang WW, Peacock CS, Matlashewski G. PLoS. Negl. Trop. Dis. 2008; 2:e248. [PubMed: 18545684]
47. Silverman JM, Chan SK, Robinson DP, Dwyer DM, Nandan D, Foster LJ, Reiner NE. Genome Biology. 2008; 9(2)
48. Shao D, Han Z, Lin Y, Zhang L, Zhong X, Feng M, Guo Y, Wang H. Acta Trop. 2008; 106:9–15. [PubMed: 18262164]

Europe PMC Funders Author Manuscripts

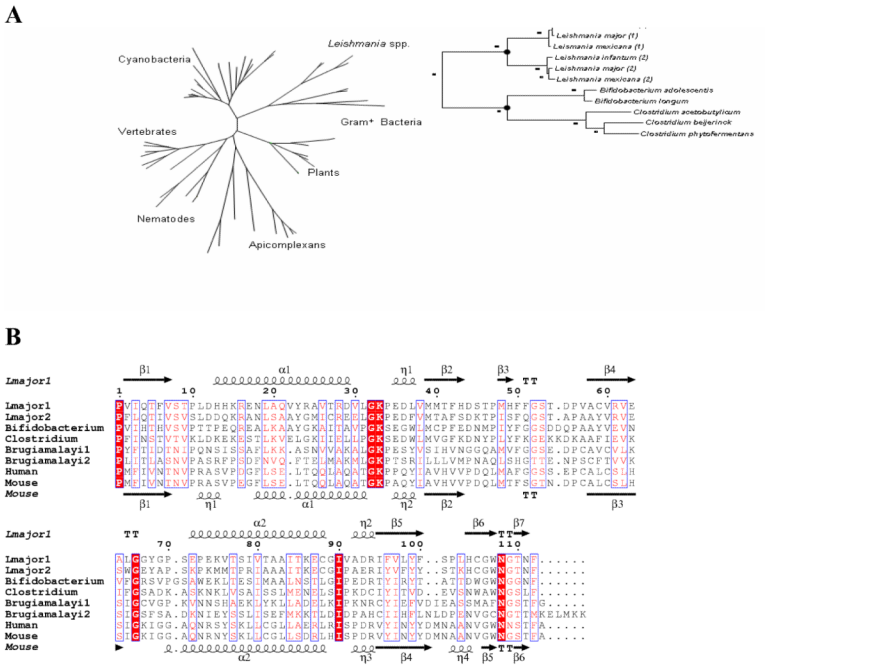

Figure 1. Sequence alignments and phylogenetic reconstruction

(A) An unrooted neighbour-joining phylogenetic tree of MIF protein sequences. For clarity, the clade containing *Leishmania* sequences has been shown in detail. A full phylogram including percentage bootstrap values is included in supplementary data 4. (B) Alignment of the sequences of MIF-like proteins from *Leishmania major*, *Bifidobacterium longum*, *Clostridium acetobutylicum*, *Brugia malay*, human and mouse. Conserved residues are highlighted by a red background and similar residues are indicated by red text and boxed in blue. The secondary structure elements of *Leishmania* MIF1 and mouse MIF are shown above and below the sequence alignments respectively.

Europe PMC Funders Author Manuscripts

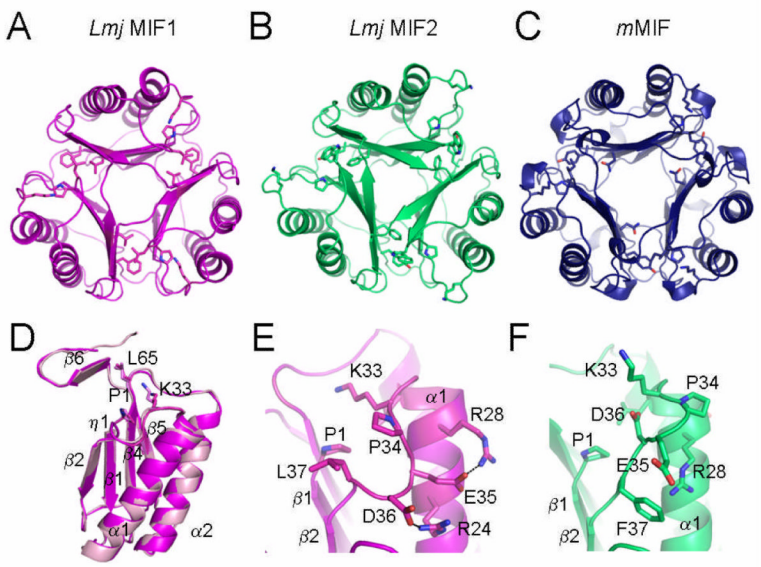

Figure 2. Structures of *Leishmania major* MIF1 and MIF2

(A) LmjMIF1 trimer, (B) LmjMIF2 trimer and (C) mouse MIF in cartoon representation; catalytic residues are highlighted by sticks. (D) An overlay of a monomer of LmjMIF1 with a N-terminal hex-His tag (magenta) and a C-terminal tag with the secondary structure elements labelled. (E) Close up of the tautomerase active site of LmjMIF1 showing the catalytic residues Pro1 and Lys33, the β turn formed by residues Pro34-Leu37 and the salt bridges between Arg24 and Asp36, and between Arg28 and Glu35 (F) The tautomerase active site of LmjMIF2. The alternative conformation of the linker region Glu30-Phe37, which contains the conserved GKP motif, removes Lys 33 from the active site.

Europe PMC Funders Author Manuscripts

Europe PMC Funders Author Manuscripts

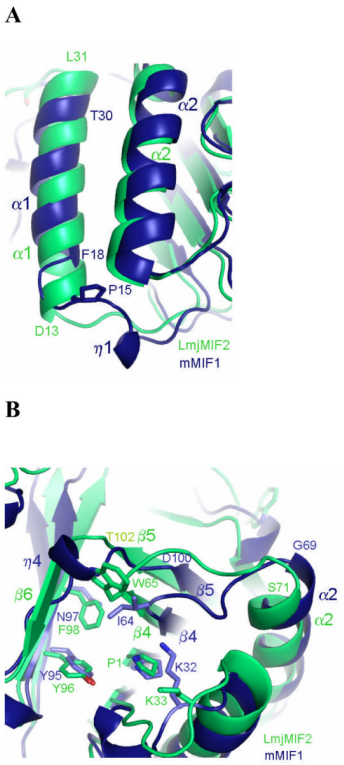

Figure 3.

(A) *Leishmania* MIFs have an extended α-1 helix compared with mouse MIF (B) The 64-71 loop has inherent flexibility and residues 100-107 form a β-strand in LmjMIFs but a η-helix in mouse MIF.

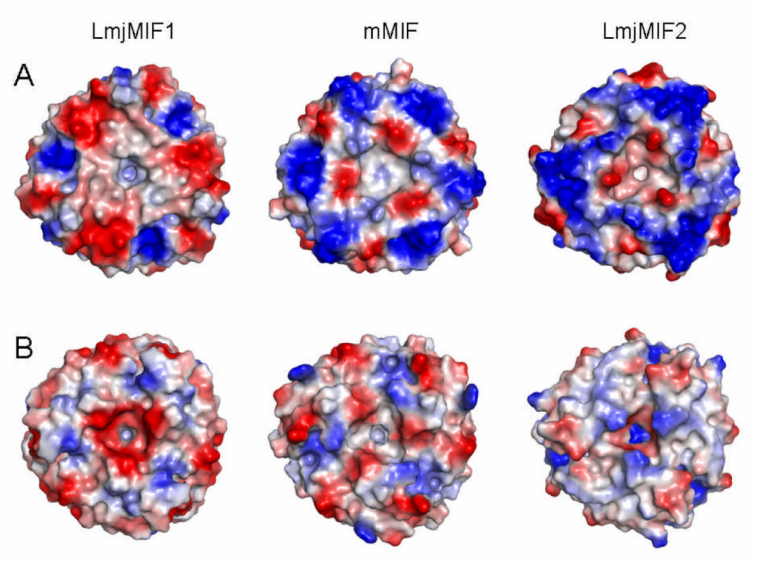

Figure 4.
Electrostatic potential surfaces of the *Leishmania* MIF and the mouse MIF structures. Positive charge is indicated in blue whereas red indicates negative charge. The views from the top and bottom of the trimers are shown in (A) and (B) respectively.

Europe PMC Funders Author Manuscripts

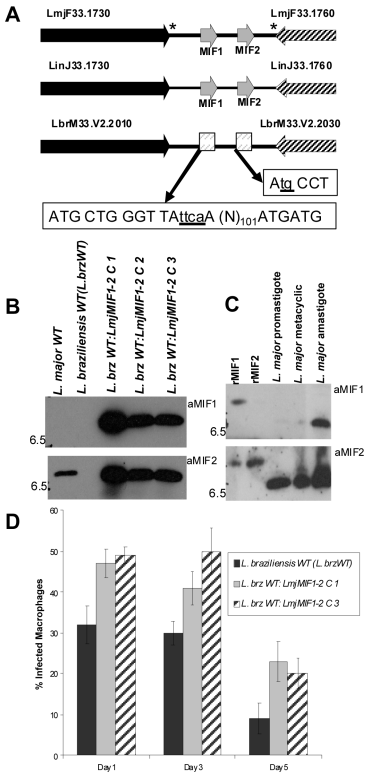

Figure 5. Expression of MIF in *Leishmania*

(A) Schematic representation of the MIF locus in *L. major* (LmjF) *L. infantum* (LinJ) and *L. braziliensis* (LbrM). Grey arrows represent intact *MIF* genes. Pseudo *MIF* locus in LbrM shows nucleotides present in LmjF and LinJ but missing from LbrM in lower case and underlined. (B) Western blot of *L. major*, *L. braziliensis* and *L. braziliensis* clones expressing LmjMIF1 and LmjMIF2 probed with anti-MIF1 and anti-MIF2 antibodies. (C) Western blot of rLmjMIF1 or rLmjMIF2 (50 pg each) or whole cell lysates from *L. major* multiplicative promastigotes, metacyclic promastigotes and amastigotes (10 μg each). (D) *L. braziliensis* WT:MIF1-2 Clone 1 (C1) and 3 (C3) were used to transfect BALB/c macrophages at a 10:1 ratio and infectivity was measured by Giemsa staining and counting under a light microscope 1, 3 and 5 days post-infection. The data are means +/− SD from three independent experiments.

Table 1

X-ray diffraction data and refinement statistics

Crystal	LmjMIF1 (N-terminal His_6 tag)	LmjMIF1 (C-terminal His_6 tag)	LmjMIF2 (N-terminal His_6 tag)
Space group	H3	P2(1)	P6(3)22
Cell dimensions	a,b=52.32Å, c=97.94Å α=β=90°, γ=120°	a=39.1Å, b=84.2Å c=48.2Å, α=γ=90°, β=109.8°	a,b=53.96Å, c=138.9Å α=β=90°, γ=120°
Mosaicity	0.45	0.89	0.50
Molecules per ASU	1	3	1
Matthews Coeff. ($Å^3Da^{-1}$)	1.76	1.99	1.95
Solvent (%)	30.8	38.4	37.1
Resolution (Å)	25-1.8 (1.9-1.8)	39.9-2.6 (2.74-2.6)	38.8-1.9 (2.0-1.9)
R(merge)	0.069 (0.121)	0.164 (0.674)	0.089 (0.362)
Total no. of reflections	52481 (4357)	33734 (4970)	105380 (11582)
No. of unique reflections	9160 (1242)	9130 (1333)	10155 (1430)
<I>/σI	20.9 (7.2)	8.6 (1.9)	21.2 (5.7)
Completeness %	98.8 (93.4)	99.9 (100.0)	100.0 (100.0)
Multiplicity	5.7 (3.5)	3.7 (3.7)	10.4 (8.1)
R/R(free)	0.192/0.255	0.250/0.327	0.228/0.278
Average B factor	18.18	35.1	21.50
Rmsd Bond	0.021	0.019	0.021
Angle	2.42	1.96	2.04
Chiral	0.123	0.120	0.185
Ramachandran core(%)	93.7	83.7	87.9
allowed (%)	5.3	14.3	10.1
generous (%)	1.1	2.0	2.0
disallowed (%)	0.0	0.0	0.0

Europe PMC Funders Author Manuscripts

Table 2

Tautomerase activity of C-terminal His_6 tagged MIF proteins. SEM is the standard error of the mean of three replicates.

Protein	Specific Activity (μmol s^{-1} mg^{-1}) +/− SEM
Mouse MIF	2011 +/− 270
LmjMIF1	76 +/− 3.2
$LmjMIF1^{P1G}$	<3
LmjMIF2	<3
$LmjMIF2^{P1G}$	<3

Europe PMC Funders Author Manuscripts

Table 3

Tautomerase active site residues of mouse and *L. major* MIFs.

mMIF	LmjMIF1	LmjMIF2
P1	P1	P1
K32	K33	K33
I64	L65	W65
Y95	F96	Y96
N97	L98	F98